A&A 598, A6 (2017)
DOI: 10.1051/0004-6361/201527736

Astronomy & Astrophysics

Latitude dependence of the solar granulation during the minimum of activity in 2009

R. Muller[1], A. Hanslmeier[2], and D. Utz[2]

[1] Institut de Recherche en Astrophysique et Planétologie de l'Observatoire Midi-Pyrénées, Université de Toulouse, CNRS; section Observatoire du Pic du Midi, 57 avenue d'Azereix, 65008 Tarbes, France
e-mail: muller@ast.obs-mip.eu
[2] Institut für Physik, Karl-Franzen Universität Graz, Universitätsplatz 5, 8010 Graz, Austria
e-mail: arnold.hanslmeier@uni-graz.at

Received 13 November 2015 / Accepted 30 September 2016

ABSTRACT

Context. Knowledge of the latitude variation of the solar granulation properties (contrast and scale) is useful to better understand interactions between magnetic field, convection, differential rotation, and meridional circulation in the solar atmosphere.
Aims. We investigated the latitude dependence of the contrast and scale of the solar granulation, with the help of HINODE/SOT blue continuum images taken in the frame of the HOP 79 program, along the central meridian and along the equator on a monthly basis in 2009 during the last solar minimum of activity.
Methods. We selected the sharpest images in latitude and longitude intervals. The selected images in all the N-S and E-W scans taken in 2009 were combined to get statistically reliable results.
Results. The contrast of the solar granulation decreases towards the poles and the scale increases, but not regularly since a perturbation occurs at around 60° where both quantities return close to their values at the disk center.
Conclusions. Such a latitude variation in a period of minimum of activity (2009), is probably not due to magnetic field, neither the quiet magnetic field at the surface, nor the strong magnetic flux tubes associated with active regions, which could be embedded more or less deeply in the convection zone before they reach the surface. The decrease in contrast and increase in scale towards the pole seem to be related to the differential rotation and the perturbation around 60° to the meridional circulation.

Key words. Sun: granulation – Sun: magnetic fields – Sun: rotation – Sun: interior – Sun: evolution

1. Introduction

The differential rotation, the magnetic field, and the meridional circulation of the Sun vary with latitude and depth. As a consequence, the Sun's physical structure is latitude dependent and at the surface it is expected that the properties of the solar granulation are also latitude dependent. Investigating the latitude variation of the granulation should thus help us to better understand the global properties of the Sun mentioned above and their mutual interactions. Moreover, variations of the solar turbulence and/or solar structure below the surface are often invoked to explain p-mode frequency shifts and m-dependent frequency splitting changes related to the solar cycle and to the latitude (Kuhn 1988, 1993, 1998, 2000;Libbrecht & Woodard 1990; Basu & Antia 2000; Houdeck et al. 2001; Dziembowski & Goode 2005).

Rodriguez et al. (1992) published the only latitude variation of the solar granulation we know. A lower contrast, a smaller mean wavenumber and a steeper center-to-limb variation of the contrast were found in the central meridian than at the equator, the effect being more pronounced around 40°. This means that the intrinsic contrast of the solar granulation decreases with latitude, reaching a maximum around 40°, and that the intrinsic scale increases, also reaching a maximum around 40°. Closer to the poles the results are uncertain. Prior to this finding, the C-shape of photospheric lines, which is due to the asymmetry of the upward and downward granular flow, was also found to be latitude dependent by several authors (Beckers & Taylor 1980; Brandt & Schröter 1982; Andersen 1984; Cavallini et al. 1985), suggesting that the granular convection changes with latitude.

There are further indications that the properties of the photosphere change with latitude, which may be related to the granulation. A temperature excess of the solar surface derived from limb profile measurements was found in active latitudes; it changes with the same time scale as the magnetic field (Kuhn et al. 1988; Kuhn & Schüssler 2000); in a period of minimum activity (1996), the temperature was found to decrease from the equator to the poles, with a minimum occurring near 50°–60° (Kuhn et al. 1998). On the other hand, Duvall et al. (1996) reported a sound speed increase in the active latitudes, not only in areas with sunspots and faculae, but also in the quiet atmosphere in between active centers which, according to Kuhn & Stein (1996), can be explained by a significant temperature excess below the photosphere. Antia et al. (2001), found a significant excess in sound speed at a depth around $r = 0.92\ R_\odot$ and at a latitude around 60°. The shape of the Sun is not a perfect sphere; it changes in response to gravitation, internal rotation, convection, and magnetic field. Actually, it is found to be slightly oblate and hexadecapoloidal. From recent accurate measurements taken with space telescopes, the oblateness amounts to about 8 mas (Emilio et al. 2007, 2009; Fivian et al. 2008; Kuhn et al. 2012). It is found to be constant over the activity cycle by some authors (Kuhn et al. 2012), but found to increase with decreasing activity by some others (Egidi et al. 2006; Djafer et al. 2008).

The hexadecapolar shape, previously detected by Lydon & Sofia (1996) and Kuhn et al. (1998), and confirmed more recently by Emilio et al. (2007, 2009), seems to vary with the cycle (Kuhn et al. 2012).

In this paper, we investigate the latitude dependence of the solar granulation using continuum images taken on a nearly monthly basis with the SOT 50 cm telescope on board the Hinode satellite. They form a unique set of seeing free high resolution images along the equator and the central meridian. Unfortunately, a significant number of these images have been blurred by instrumental thermic effects and/or inaccurate focusing (Sect. 2), which requires a careful selection of the sharpest images (Sect. 3). The results obtained in 2009, right in the middle of the extended minimum of activity between cycles 23 and 24, are presented in Sects. 4 and 5 and discussed in Sect. 6.

2. Observations: The Hinode/HOP 79 program

For this investigation, we used the images taken in the blue continuum at 450.45 nm by the Hinode/SOT 50 cm telescope Tsuneta et al. (2009), in the frame of the Hinode Observing Program 79 (HOP 79), the "irradiance program". This program is aimed at better understanding the variation of irradiance with rising flux levels in the photosphere throughout the ascending phase of Cycle 24 and beyond. It consists of sets of scans covering all latitudes along the north-south (N-S) direction taken on a nearly monthly basis since January 2009. It includes filtergrams taken at various wavelengths by the Filtergraph Instrument (SOT/FG) and spectroheliograms taken with the SOT/SP instrument. Originally, each set included one N-S scan along the central meridian and two east-west (E-W) scans at +15° and –15° from the equator, close to the active latitude belts; in May 2009 an E-W scan crossing the disk center was added, which can be used as a reference for the N-S variations, making HOP 79 well suited for investigating the latitude variation of the solar granulation. Because the E-W disk scans are always performed close to the solar equator, they are referred to as E-W equatorial scans or, more simply, E-W scans throughout the paper.

Rectangular images of size 224″ × 112″ are provided by two 2048 × 2048 square pixels adjacent cameras of pixel scale 0.″055, but for HOP 79 the images are binned providing a working pixel scale of 0.″11. For our granulation investigation, only the N-S central meridian and the E-W equatorial scans were used. The N-S solar diameter is fully covered by adjacent images taken on 20 pointing positions spaced by 100″; the equatorial diameter is fully covered by 10 pointing positions spaced by 200″. In order to have the same foreshortening effects in the images taken near the polar and the equatorial limbs, only the central 1024 × 1024 pixels subfields of the N-S scan images were used. The two eastern and western 1024 × 1024 subfields of equatorial images were processed separately. Two images separated by about 3 min were taken in each pointing position, which means that 40 images of 1024 × 1024 pixels (112″ × 112″) are available along each direction to investigate the latitude variations of the contrast and scale of the solar granulation. The E-W variations were used as reference variations because the granulation is uniform around the equator (Muller et al. 2011). Their shapes come from the combination of several effects: foreshortening, radiative transfer, and instrumental aberrations (blurring and image deformation); moreover, increasing heights are seen when approaching the limbs. The variations of the granulation contrast and scale as a function of the distance to the disk center and of the solar latitude can be found by comparing the N-S to the E-W variations. We see below that we were faced with a major problem: when comparing the images taken at the same distance or nearly at the same distance from the disk center, we found that they are not always of equal sharpness. Consequently, the crucial point in this investigation is the careful and objective selection of the sharpest images.

In the following, we investigate the latitude dependence of the solar granulation in 2009, during the extended minimum between cycles 23 and 24. Twelve N-S scans are available for this year, but only four E-W scans, because the equatorial scans were included in HOP 79 only in May 2009. In order to improve the statistical accuracy we added the nine E-W scans taken in 2010 to those taken in 2009. They can be used together with the 2009 scans because at the disk center the granulation did not change between 2009 and 2010 (Muller et al. 2011).

3. Image analysis

All images were calibrated with the standard solar reduction software distributed under SSWIDL (Solar SoftWare Interactive Data Language), which corrects bad pixels, readout errors, dark current, and flat field. The mean image intensity decreases by a factor of 2 between the disk center and 928″ from it, where the most distant analyzed field of view is centered. The large-scale brightness inhomogeneities – which close to the limbs are mainly due to the limb darkening – were removed in each image (by subtracting a second-order polynomial fitting), before computing the contrast and the scale of the solar granulation. In this work, the granulation contrast is simply the standard deviation of these filtered images, whose mean intensity was set to 1. The granulation scale is derived from the autocorrelation function (ACF): it is defined as the mean of the ACF values obtained for a shift of 4 pixels (0.″44) in the directions parallel and perpendicular to the limbs (0.″44 is close to the ACF half width (ACFHW)). In the following, the scales derived from ACFs computed in the directions parallel and perpendicular to the limbs are called parallel scale and perpendicular scale, respectively; their mean is defined as the granulation scale. We do not derive the contrast and the scale from the granulation power spectra as was done in Muller et al. (2011) because the final calculations are performed on rectangular subfields of 1024 × 512 pixels instead of square fields of view. However, we checked on several scans that the results obtained with the two methods were nearly identical. Each N-S and E-W scan was processed individually. The analysis began by the visual inspection of all the images of the investigated scan in order to detect and remove those which contain dark columns, sunspots, or abnormal granulation[1]. Removing these images ensures that the selected images were taken in the quietest areas of the Sun. In addition, some images are obviously blurred, certainly because of focusing problems; they were also removed at this step. Then, for each scan, the limb-to-limb variation of the contrast and of the various scales (mean, parallel, and perpendicular, as defined above) were plotted as in Fig. 1. In all variations, several images of contrast and scale were found to depart from a regular variation: their contrast falls below and their scale above the regular variation (for example the images at the position –543″ and –444″ in Fig. 1c), suggesting that they might be slightly blurred. When the blurred images are mostly located in the same hemisphere, the variations appear asymmetric relative to the disk center, as for example in Fig. 1a where the variation of the contrast is steeper in the southern hemisphere,

[1] Abnormal granulation is a granulation area that appears smeared by the presence of many magnetic bright points in the intergranular lanes; in the quiet Sun they belong to the remnant of an active region.

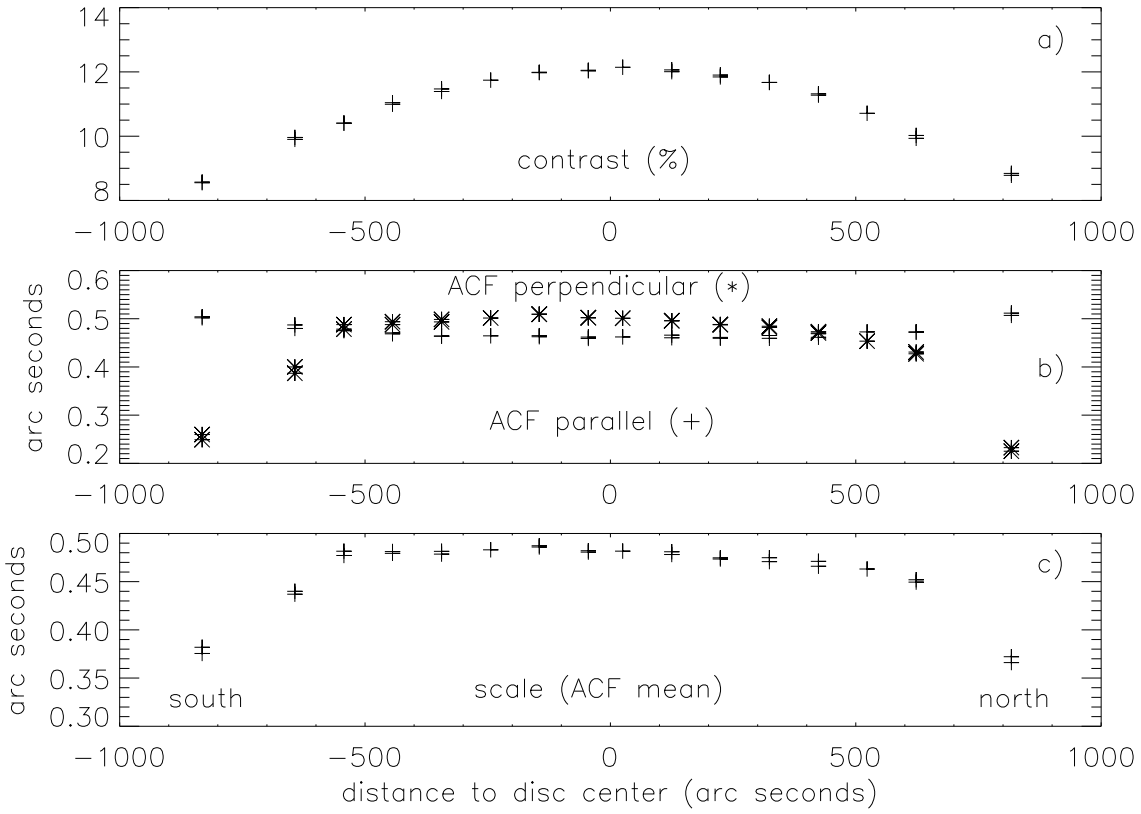

Fig. 1. Variation of the contrast panel **a)** and the scale panel **c)** of the solar granulation (defined in Sect. 1) for the Hinode/SOT HOP 79 north-south scan of December 21, 2009. The field of view of the images is 1024 × 1024 pixels (112″ × 112″). Panel **b)** shows the variations of the "parallel scale" (+) and "perpendicular scale" (*) derived from the autocorrelation functions (ACFs) computed in the directions parallel and perpendicular to the polar limbs. "ACF mean" is the mean between ACF parallel and ACF perpendicular. A few images with dark columns and those containing the limbs have already been removed. The images at positions –543″ and +623″, which depart from a regular variation in panel **c)** and which, visually, appear clearly out of focus, will be removed.

and in Fig. 1c where the scale variation is irregular; at least for the equatorial variations, such asymmetries cannot be of solar origin. The blurring may be caused by temperature variations of the spacecraft when it is shifted from one pointing position to another, or by inaccurate focusing.

It thus became evident that the sharpness of all images should be checked carefully and only the sharpest ones selected in order to get a homogeneous set of images of high quality. In Muller et al. (2011), where all the granulation images were taken at the disk center, the selection of the sharpest images could be made in a quantitative manner, using one parameter based on the contrast and on the scale of the solar granulation, both derived from the power spectrum of the intensity fluctuations. When an image had this parameter lower than the reference value, the image was selected, otherwise it was removed. Unfortunately, such a quantitative procedure cannot be used for our center-to-limb investigation, because the reference parameter would vary as a function of the distance to the disk center. Instead, we used the contrast and the scale of the sharpest images as reference parameters. However, the first step of the selection procedure was purely visual. We compared visually the sharpness of the images taken in intervals of width of 100″, at increasing distances from the disk center where the foreshortening is nearly the same, both along the equator and the central meridian. At this step the sharpest images were selected, some blurred images were removed, and some doubtful images that seemed to be only slightly blurred were kept to be checked quantitatively in the next step of the selection procedure.

The contrast and the scale of all the selected images in each latitude interval of the 12 N-S scans were then plotted versus the distance to the disk center (Fig. 2). Afterwards these two variations will be used as reference variations for the contrast and for the scale. The dispersion of the individual values in Fig. 2 is due to the statistical variation of the granular pattern and to a residual difference of sharpness of instrumental origin. Then the contrast and the scale of the images selected visually in each monthly N-S scan, as described above, were overplotted on the reference variations (Fig. 2). If the contrast or the scale – or both – of a visually doubtful image departed from the reference plot, i.e., if the contrast was lower than that of the images taken at nearly the same latitude or if the scale was higher – or both – the image was discarded (for example, the images at positions −543″, −444″, +523″, and +623″ in Fig. 2 will be removed later on). On the other hand, some images that appeared doubtful to us, visually, but have in fact a contrast and a scale that fall inside the dispersion, were accepted as selected images. With this new set of reference selected images, the image quality control process was repeated for each N-S 2009 scan. A few more images were then accepted or removed. This selection procedure was also used to select the sharpest images of the 13 E-W 2009–2010 scans. The final selected images were then used to compare the N-S and E-W contrast and scale variations: a difference would reveal a change in the solar granulation with latitude.

Figure 1 also shows that close to the disk center, where the foreshortening is negligible, the granulation appears elongated in the images from the program HOP 79; in the case of the

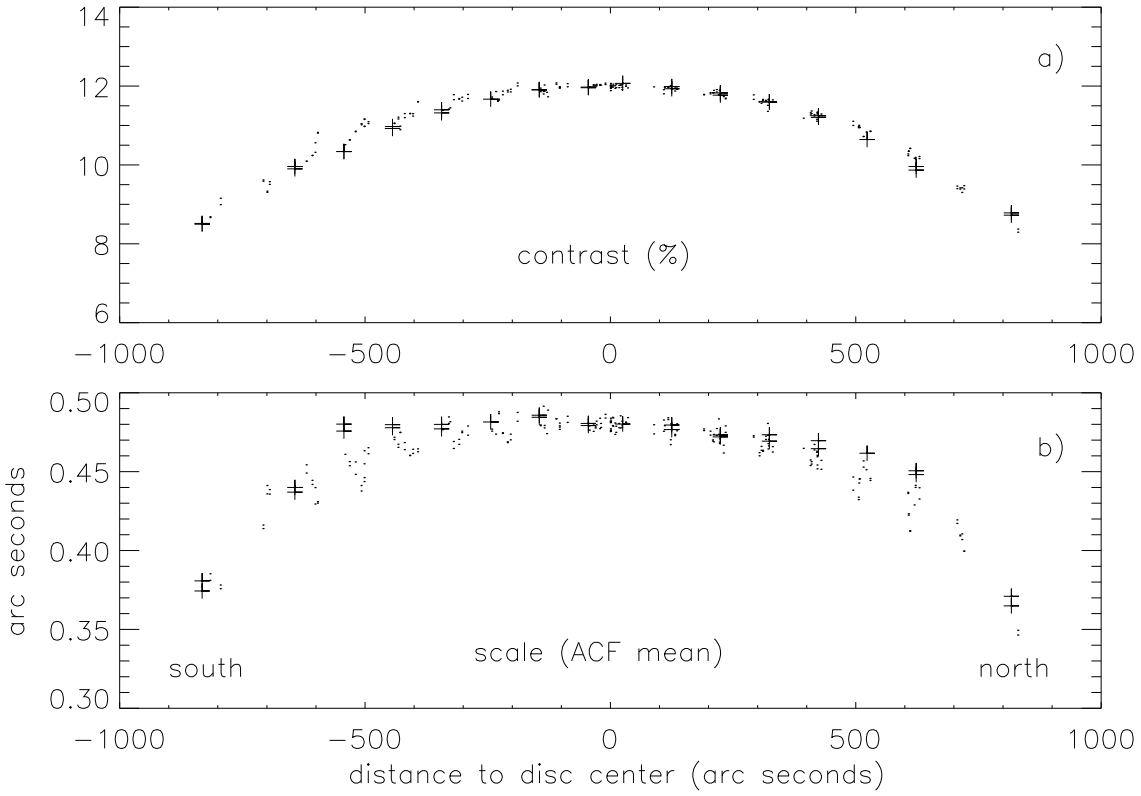

Fig. 2. Variation of the contrast (panel **a**)) and the scale (panel **b**)) of the solar granulation of the N-S scan of December 21, 2009 (+), compared to those of all the images selected visually in the 12 N-S scans taken in 2009 (.). The images at positions –543″, –444″, +523″, and +623″ will be removed because their contrast is below that of the selected images and their scale above, indicating they are blurred, as confirmed by a visual check.

N-S scan shown in Fig. 1b, the ACF parallel to the polar limbs is smaller than the ACF perpendicular to them, which means that, for instrumental reasons, the granulation is elongated in the N-S direction. The granulation appears elongated in most E-W and N-S scans, preferentially in the N-S direction. The elongation may be as high as 10% in the extreme cases. It is of 5% on average for the N-S scans and of 2% for the E-W scans. Away from the disk center, the behavior of the N-S and E-W variations of ACF parallel and perpendicular to the limbs also suggests that the images taken at any distance from the disk center are elongated, again preferentially in the N-S direction. This confirms that it is appropriate to average ACF parallel and ACF perpendicular, thus minimizing the instrumental elongation, to characterize correctly the scale of the solar granulation. The granulation elongation is correlated with the granulation contrast, such that the most distorted images have the lowest contrast. Moreover, both variations exhibit a yearly modulation; the maximum of contrast is reached in May−July 2009. The yearly modulation of contrast and scale is also clearly visible in the variation of the solar granulation over the solar cycle derived, at the disk center, from images taken in the frame of the Hinode synoptic program (Muller et al. 2011, and in prep.). It thus seems that the yearly modulation of the granulation contrast is a consequence of a yearly variation of astigmatism, which is probably due to a deformation of the primary mirror, caused by a yearly variation in the temperature of the supporting pads (Ichimoto, priv. comm.).

When the images are retrieved from the Hinode DARTS data base, the coordinates of their center are given in arc seconds from the disk center in the N-S and E-W directions, but verification of these coordinates on the images containing a limb revealed that they are incorrect. For these images, the correct coordinates were obtained using the limb as a reference. The difference between the real and the given coordinates can be as high as 50″; on average, it is of −15″ at the south limb, +11″ at the north limb, −8″ at the east limb, and +13″ at the west limb. A negative difference means that the real limb coordinate is closer to disk center than the given one. For each scan, the position difference was determined for the N and S (E and W) limb images. The correction for the other images of the scan was obtained by interpolating the corrections made for the two limb images.

As several images were removed from each scan, sometimes more than half of them, it was not possible to compare a single N-S scan with a single E-W scan. To get statistically reliable results, we combined all the selected images from the 12 N-S scans made in 2009 on one side, and all the selected images from the 13 E-W scans made in 2009 and in 2010 on the other side. In total, 283 images, out of 480, were selected in the N-S scans (about 60%), and 180 out of 260 (about 70%) in the E-W scans. In order to increase the resolution along the polar and equatorial axis, the FOV was split into two subfields in the direction parallel to the limbs. Closer to them, we used even narrower FOVs, of 384 pixels (42″) in width because of the steep variation of the granulation appearance towards the limb. These narrow FOVs were centered at 928″ from the disk center and the distance of their outer border was at 10″ from the limb (Fig. 3). At the extreme limb, the granulation vanishes too much to give reliable contrast and scale values. Thus finally, the granulation contrast and scale were computed in 566 and 721 rectangular subfields along the N-S and E-W solar axis, respectively.

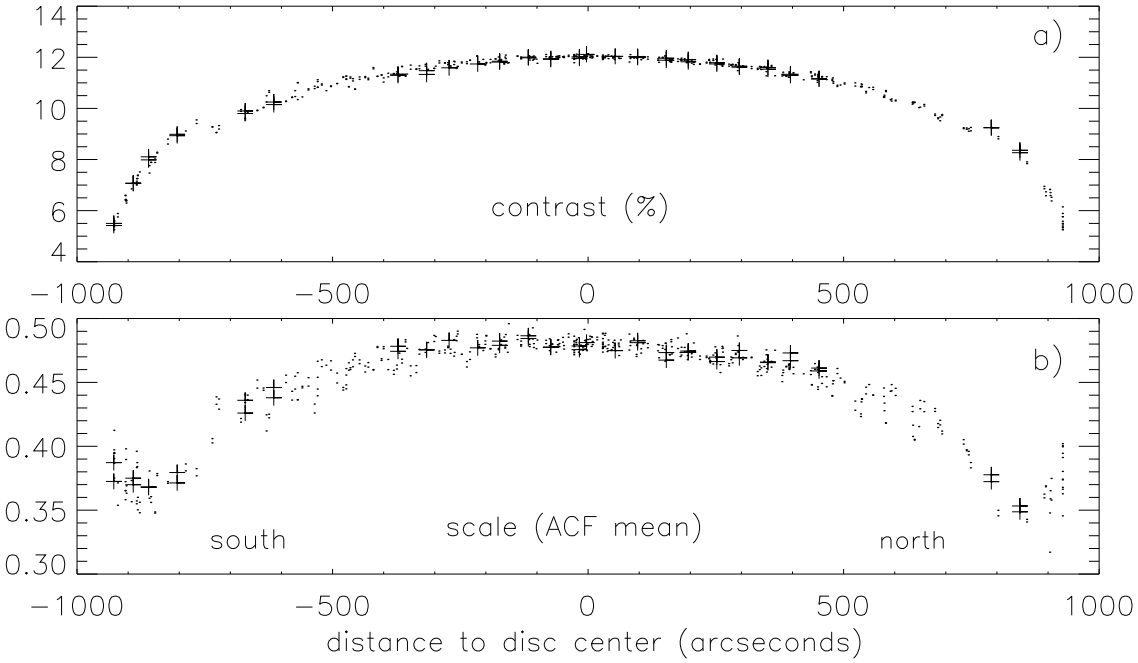

Fig. 3. Variation of the granulation contrast (panel **a)**) and scale (panel **b)**) of the selected images in the N-S scan of December 21, 2009 (+), compared to the variations of *all* the selected images in the 12 N-S scans made in 2009. The blurred images at positions –543″, –444″, +523″, +623″ in Fig. 2 are removed. Here, the selected images are divided in two subfields 1024 × 512 pixels (112″ × 56″), in the direction parallel to the polar limbs, in order to increase the scan resolution. Moreover two subfields extracted from the images containing the southern limb are added, one of size 1024 × 512 pixels at the position –890″, the other one, of smaller size, 1024 × 384 pixels, centered at the position –928″; the outer boundary of this subfield is at 10″ from the limb (no subfields have been added close to the northern limb, because the corresponding images are slightly blurred).

4. Latitude variation of the granulation contrast

The contrast computed in the 1024 × 512 pixels FOVs of all the images selected in the 13 E-W and the 12 N-S scans is plotted in Fig. 4a as a function of the distance to the disk center, expressed in arcseconds. Each scan is normalized to the same reference contrast of 12% at the disk center. The normalization is necessary because the contrast of the granulation measured with HINODE/SOT varies with time for instrumental reasons (Muller et al. 2011), around 12%. The dispersion of the individual values is due to the statistical variation of the granular pattern and to a residual difference in sharpness of the selected images. The photometic noise is negligible. Eighth-order polynomials, computed separately in each hemisphere – east, west, north, and south – best fit the variations of the individual values as they provide the smallest standard deviation of the individual values with respect to the polynomials. The polynomials are overplotted on the individual points in Fig. 4a. The contrast decreases from the disk center towards the limbs because the smallest features vanish under the combined effect of foreshortening, instrumental diffraction, and radiative transfer; moreover, the smallest granules do not overshoot as high as the largest ones (Espagnet et al. 1995; Berrilli et al. 2002). The E-W variation must be symmetric relative to the disk center because the granulation is homogeneous around the equator (Muller et al. 2007, 2011). It is actually found to be nearly symmetric here, as expected. The N-S variation is also found to be nearly symmetric. The fact that both variations are symmetric means that the selection of the sharpest images has been made satisfactorily, and that the instrumental aberrations are nearly identical in each hemisphere along the central meridian and along the equator. It thus appears that the north-south symmetry of the variation of the granulation contrast was very likely an intrinsic property of the Sun during the minimum of magnetic activity in 2009.

The 8th order polynomial fits are used to compare the N-S meridional variation to the reference E-W equatorial variation (Fig. 4a). It must be noted here that, because all the selected images taken in 2009 in the N-S direction are used to derive the 8th order N-S meridional variation, the angle B_0 is zero on average, and no correction for this angle has to be made to get the correct latitude position from the corresponding distance to the disk center. The latitudinal variation differs significantly from the reference equatorial variation, revealing a latitude dependence of the contrast of the solar granulation (Figs. 4a and b). Since the northern and southern variations are nearly identical (Fig. 5a), the two hemispherical variations can be averaged in order to reduce the uncertainties. This is done by fitting an 8th order polynomial to the individual values folded in the same hemisphere. The averaged E-W polynomial is obtained in the same way. The N-S and E-W averaged 8th order polynomials and their relative difference (the difference divided by the contrast at the same latitude) are plotted in Figs. 5b and c. The relative difference N-S/E-W (Fig. 5c) shows that the contrast of the solar granulation decreases nearly regularly from the disk center to a distance of 660″ (latitude 45°) before returning to a value close to that at the disk center at a distance of 825″ (latitude 60°); then it decreases steeply towards the poles, at least to the distance reached by our investigation (930″), which corresponds to a latitude of 75°. At the highest latitude reached by our investigation (75°), the contrast is found to be 4% smaller than at the disk center. Because of the finite resolution of the observations, it is a lower value. A plateau is also found where the contrast is nearly constant, between 300″ and 450″, corresponding to the latitude interval 18°–28°. This plateau may be real because it is visible in

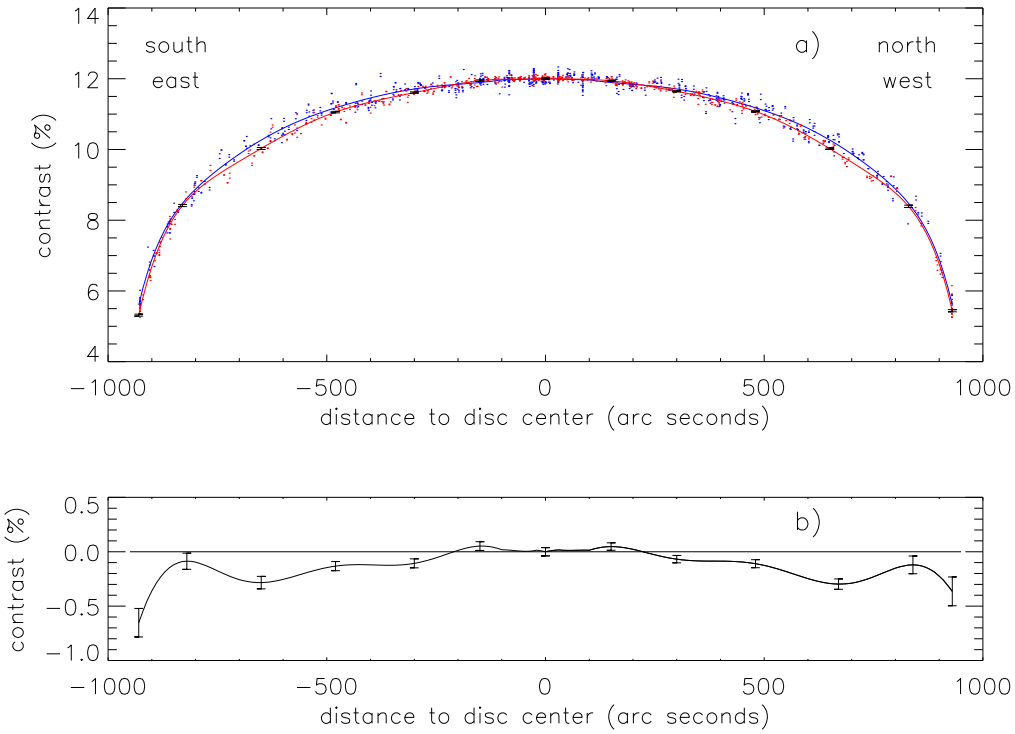

Fig. 4. Panel **a**): comparison of the N-S (red) and E-W (blue) variations of the granulation contrast: individual selected images (dots); 8th order polynomial fits, computed separately in the N, S, E and W hemispheres (full lines). The error bars are weighted standard deviations of the individual values with respect to the polynomial fits, computed along the polynomials. They are only plotted in a few positions on the N-S polynomials, but they are as short on the E-W polynomials. The error bars are very short, because a large number of individual values are involved in the computation and their dispersion is rather small. Panel **b**): difference between the N-S and E-W variations, relative to the granulation contrast at the same distance from the disk center. The errors along the difference between the N-S and E-W polynomials are the sum of the N-S and E-W errors.

both hemispheres and because the N-S and E-W variations are symmetric relative to the disk center. The symmetry also indicates that the instrumental aberrations, if any, are nearly identical along the central meridian and along the equator.

5. Latitude variation of the granulation scale

The N-S and E-W variations of the scale of the granulation, derived from the same set of selected images used to derive the contrast variations, are plotted as a function of the distance from the disk center in Fig. 6. For the same reason as for the contrast, each scan is normalized to the same reference scale of 0.″45 at the disk center. Also as for the contrast, 8th order polynomials are overplotted, which best fit the individual values. They are computed separately for the N, S, E, and W hemispheres. The granulation scale decreases outward from the disk center because of foreshortening, but beyond 900″ (latitude 70°) for the E-W variation and beyond 870″ (latitude 65°) for the N-S variation, it starts to increase, probably because the smallest features vanish. A close inspection of the granulation near the limb actually reveals that the large granules, which appear very elongated there, do not show any fine features as they do at the disk center. To our knowledge, such an increase in scale towards the limb has never been reported before. Neither the N-S nor the E-W variation is symmetric relative to the disk center. As for the contrast, the E-W variation should be symmetric; the asymmetry is due to the instrumental image distortion discussed in Sect. 3, which elongates the granules preferentially in the N-S direction. For this reason, it is not possible to compare the full limb-to-limb latitudinal and equatorial variations as was done for the contrast. Instead, the comparison is made between the north-south and east-west folded variations (Fig. 7a), which are obtained with the same method as for the contrast. Figure 7b shows their difference as a function of the distance from the disk center, relative to the granulation scale at the same distance. Figure 7 clearly shows that the scale of the granulation is latitude dependent. It increases from the disk center to a distance of 660″ (latitude 45°) before returning, as for the contrast, to the disk center value at a distance of 825″ (latitude 60°); then it increases steeply towards the poles, at least to the distance reached by our investigation (930″, which corresponds to a latitude of 75°). The plateau between 300″ and 450″, which is visible in the contrast variation, is less clear here, although the variation is slightly flatter in this range than outside it.

At the highest latitude reached in our investigation (75°), the scale is 7% larger than at the disk center. This difference is significantly larger than the granule elongation of instrumental origin at the disk center (3.5%) and larger than the error bars. Thus the increase of size of the granulation towards the limb is very likely real, but its exact amplitude is still not known precisely because of the uncertainties mentioned above, and of the finite resolution of the observations.

6. Discussion and conclusions

The difference in variations of the granulation contrast and scale between the central meridian and the equator reveals that, actually, the solar granulation is latitude dependent. During the extended minimum of activity in 2009, the contrast was decreasing and the scale increasing from the disk center to the latitude of

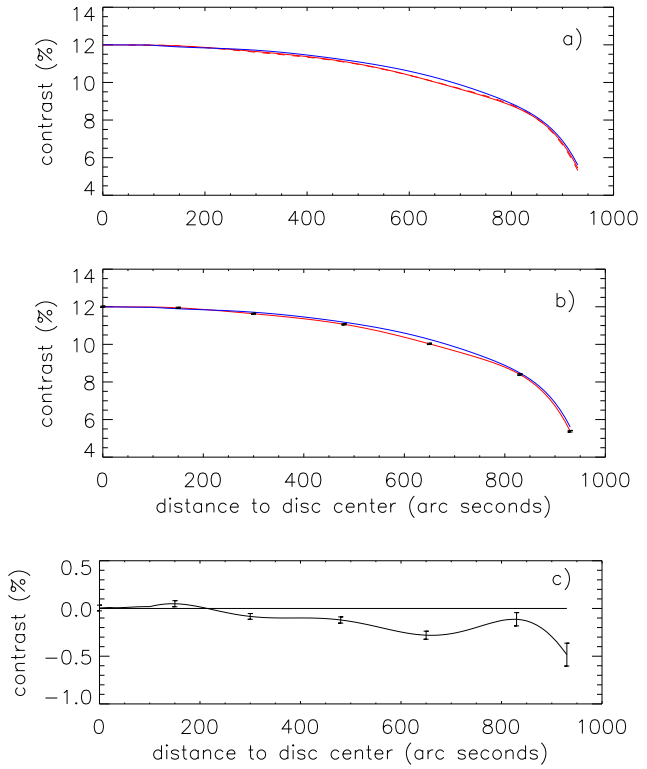

Fig. 5. Panel **a)**: comparison of the contrast variations along the northern central meridian (red solid line), the southern central meridian (red dashed line), and along the equator, averaged between the eastern and western hemispheres (blue line). Panel **b)**: comparison of the contrast variation along the central meridian averaged between the northern and southern hemispheres (red line), with the variation along the equator, averaged between the eastern and western hemispheres (blue line). Panel **c)**: difference between the N-S and E-W averages, relative to the granulation contrast at the same distance from the disk center; the error bars are derived from the dispersion of the individual values (see the caption of Fig. 4).

75° reached by our investigation, but not uniformly; a perturbation occurred near 60° where the contrast and the scale returned close to their disk center values. These variations are similar to those published by Rodriguez et al. (1992) between the disk center and 60°, although their observations were not taken during the same phase in the active cycle (minimum of activity in our case, ascending phase in theirs). Closer to the limb, the two variations are different, but the statistical accuracy is much higher in our investigation (many more available images with larger field of view). The latitude dependence of granulation we find also resembles the latitude variation of the surface temperature derived by Kuhn et al. (1987; Fig. 2b) and by Kuhn (1998; Fig. 3), from limb shape measurements around the Sun: these authors found that the surface temperature is lower at the poles than at the disk center, and is minimum at a latitude around 50°–60° at periods of minimum of activity. This suggests that the decrease in the granulation contrast away from the disk center is associated with a decrease in the surface temperature and, therefore with a decrease in convective flux (Parker 1995; Kuhn & Stein 1996). Not only are the granulation and the surface temperature found to be latitude dependent, but also the shape of the Sun, which is not perfectly spherical and changes during the activity cycle. In periods of minimum of activity a hexadecapoloidal shape is superimposed onto its oblate shape. The polar radius is smaller than the equatorial radius, while at mid-latitudes the radius is slightly larger (Emilio et al. 2007, 2009; Rozelot et al. 2009; Kuhn et al. 2012). It thus appears that – at least in periods of minimum of activity – the granulation, the surface temperature, and the shape of the Sun have similar latitude dependences and so may have the same physical origin. We also note that an excess of sound speed at a depth of around $r = 0.92\ R_\odot$ and latitude 60° was reported by Antia et al. (2001).

One explanation for the latitude variation of the granulation could be an interaction between convection and magnetic field, either with the strong magnetic field associated with active regions or with the weaker field in the quiet Sun. The numerical simulation of local magnetoconvection with a weak initial seed field performed on top of the convection zone by Cattaneo et al. (2003) shows, at the end of the simulation, that the magnetic field is located at the corners of a mesocellular pattern that is very similar in size to the mesogranulation. When a net vertical flux of increasing strength is imposed, the horizontal scale of convection decreases. The mesocellular magnetic pattern may correspond to the intranetwork (IN) magnetic field. However, Lites et al. (2014), who analyzed high spatial resolution, high polarimetric sensitivity Hinode/HOP79 magnetograms, do not find with certainty a latitudinal variation of the IN magnetic flux between the disk center and 60° during the period 2009–2013 which could have explained the latitude variation of the granulation (in fact, they infer the apparent measured increase of the IN flux towards the poles to a center-to-limb effect, not to a latitude effect). Furthermore, the NASA low resolution synoptic map (Hathaway 2010; Lites et al. 2014) does not show any significant variation between the disk center and 75° in 2009. It is important to note, however, that in this low resolution and low magnetic sensitivity synoptic map, only the elements with strong flux are detected (ephemeral active regions and enhanced network). On the other hand, the strong magnetic field which erupts at the surface in active regions and is generated at the base of the convection zone, rises nearly vertically (Caligari et al. 1995; Fan & Fisher 1996; Fan 2009; Weber et al. 2013). This means that one can never find strong magnetic fields in the convection zone away from the latitude belts and consequently, that strong fields cannot disturb the granulation at middle and high latitudes. In the synoptic map mentioned above, there is no trace of magnetic activity visible in the active belts in 2009; moreover, our results show that the granulation is not perturbed in these latitudes. Consequently, if at this phase of minimum of activity some strong magnetic field is embedded deep in the convection zone, the structure of the atmosphere close to the surface is not perturbed, which is in disagreement with the predictions of several theoretical works (Parker 1987, 1995; Kuhn 1988, 1993; Kuhn et al. 1988; Goode & Kuhn 1990). Therefore, the magnetic field (neither the quiet Sun magnetic field nor the strong magnetic field in active regions) is probably not the cause of the latitude variation of the solar granulation in the period of minimum of activity reported in this paper.

The differential rotation, which decreases from the disk center to the poles, could explain the decrease in the granulation contrast with latitude if the interaction between rotation and convection occurs deep in the convection zone, where it can be efficient enough to modify the large-scale convective pattern and the stratification of the atmosphere above; at the surface this would result in a granulation varying in latitude. Previously, Kuhn et al. (1988) also suggested that a latitudinal temperature distribution characterized by large-scale quadrupolar variations could be related to the solar differential rotation. Then the question arises about the cause of the perturbation which occurs around 60°. It could be related to the meridional

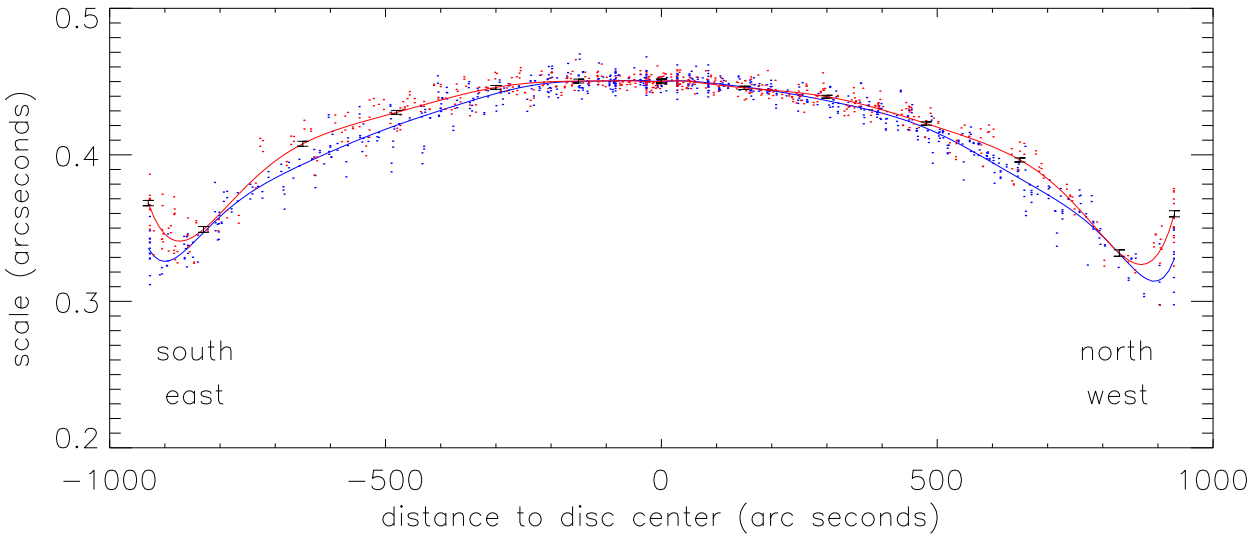

Fig. 6. Comparison of the N-S (red) and E-W (blue) variations of the granulation scale: individual selected images (dots); 8th order polynomial fits, computed separately in the N, S, E, and W hemispheres (full lines).

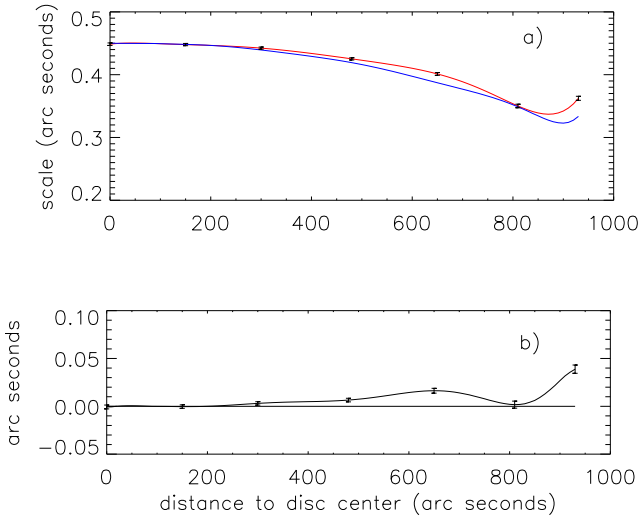

Fig. 7. Panel **a)**: comparison of the granulation scale variation along the central meridian averaged between the northern and southern hemispheres (red line), with the variation along the equator, averaged between the eastern and western hemispheres (blue line). Panel **b)**: difference between the N-S and E-W averages relative to the granulation scale at the same distance from the disk center; the error bars are derived from the dispersion of the individual values (see Sect. 4).

circulation, which moves polewards from the surface down to about 0.9 $R_\odot$, but reverses around 55°–60° to move equatorwards in deeper layers (see Fig. 3a in Zhao et al. 2013 and Fig. 4 in Jackiewicz et al. 2015). Kuhn et al. (1987, 1988) also suggested that the dip in temperature they found at 50°–60° could be related to a meridional circulation.

The size of supergranules has been found to vary with latitude, but surprisingly it decreases towards the poles while the granulation scale increases (Brune & Wöhl 1982; Rimmele & Schröter 1989; Münzer et al. 1989; Berrilli et al. 1999; Nagashima et al. 2011). As granules form just beneath the surface, supergranules form much deeper, a few tens of Mm below. The difference in latitude dependence of granules and supergranules may reflect a complicated latitude dependence of stratification in the convection zone, as suggested by the finding that, on a global scale, the atmosphere does not expand homologously over the solar cycle. For example, according to Lefebvre & Kosovichev (2005), the "helioseismic" radius varies in antiphase with the solar activity just below the surface where granules form, but the radius of the deeper layers, between 0.975 $R_\odot$ and 0.99 $R_\odot$ where supergranules form, changes in phase with the 11-yr cycle. Moreover, the "visible" diameter derived from limb brightness measurements remains constant during the cycle (Bush et al. 2010).

The main conclusion of this discussion is that the latitude variation of the solar granulation in a period of minimum of activity (2009) that we have reported in this paper is probably not due to magnetic field – neither the quiet magnetic field at the surface nor the strong magnetic flux tubes embedded more or less deeply in the convection zone. The decrease in contrast and the increase in scale towards the poles seem to be related to the differential rotation and the perturbation around 60° to the meridional circulation.

We are now investigating the latitude dependence of the solar granulation over the activity cycle from 2010 when the Sun was still very quiet to beyond the maximum of activity which occurred in 2014. This should help us to understand better why the solar granulation varies with latitude.

Acknowledgements. The authors acknowledge the support of the Austrian-French scientific exchange programme "Amadeus" (R.M. and A.H.) and the support of the Austrian Fonds zur Förderung der Wissenschaftlichen Forschung (A.H. and D.U.). They are also grateful to the Hinode team for the possibility to use their data. Hinode is a Japanese mission developed and launched by ISAS/JAXA, collaborating with NAOJ as a domestic partner, NASA and STFC (UK) as international partners. Scientific operation of the Hinode mission is conducted by the Hinode science team organized at ISAS/JAXA. This team mainly consists of scientists from institutes in the partner countries. Support for the post-launch operation is provided by JAXA and NAOJ (Japan), STFC (UK), NASA (USA), ESA, and NSC (Norway). Part of this work was done while A.H. was visiting the Midi Pyrénées Observatory and R.M. the Institut für Geophysik, Astrophysik und Meteorologie, University Graz.

References

Andersen, B. N. 1984, Sol. Phys., 94, 49
Antia, H. M., Basu, S., Hill, F., et al. 2001, MNRAS, 327, 1029
Basu, S., & Antia, H. M. 2000, Sol. Phys., 192, 449

Beckers, J. M., & Taylor, W. R. 1980, Sol. Phys., 68, 41
Berrilli, F., Ermolli, I., Florio, A., & Pietropaolo, E. 1999, A&A, 344, 965
Berrilli, F., Consolini, G., Pietropaolo, E., et al. 2002, A&A, 381, 253
Brandt, P. N., & Schröter, E. H. 1982, Sol. Phys., 79,3
Brune, R., & Wöhl, H. 1982, Sol. Phys., 75, 75
Bush, R. I., Emilio, M., & Kuhn, J. R. 2010, ApJ, 716, 1381
Caligari, P., Moreno Insertis, F., & Schüssler, M. 1995, ApJ, 441, 886
Cattaneo, F., Emonet, T., & Weiss, N. 2003, ApJ, 588, 1183
Cavallini, F., Ceppatelli, G., & Righini, A. 1985, A&A, 150, 256
Djafer, D., Thuillier, G. Sofia, S., & Egidi, A. 2008, Sol. Phys., 247, 225
Duvall, T. L., D'Silva, S., Jefferies, S. M., Harvey, J. W., & Schou, J. 1996, Nature, 379, 235
Dziembowski, W. A., & Goode, P. R. 2005, ApJ, 625, 548
Egidi, A., Caccin, B., Sofia, S., Heaps, W., et al. 2006, Sol. Phys., 235, 407
Emilio, M., Bush, R. I., Kuhn, J. R., & Scherrer, P. 2007, ApJ, 660, L161
Emilio, M., Kuhn, J. R., & Bush, R. I. 2009, in Solar and Stellar Variability: Impact on Earth and Planets, eds. A. G. Kosovichev, A. H. Andrei, & J. P. Rozelot, IAU Symp., 264, 21
Espagnet, O., Muller,R., Roudier, T., et al. 1995, A&A, 109, 79
Fan, Y. 2009, Liv. Rev. Sol. Phys., 6, 4
Fan, Y., & Fisher, G. H. 1996, Sol. Phys., 166, 17
Fivian, M. D., Hudson, H. S., Lin, R. P., & Jabran Zahid, H. 2008, Science, 322, 560
Goode, P. R., & Kuhn, J. R. 1990, ApJ, 356, 310
Hathaway, D. H. 2010, Liv. Rev. Sol. Phys., 7, 1
Houdek, G., Chaplin, W. J., Appourchaux, J., et al. 2001, MNRAS, 327, 483
Jackiewicz, J., Serebryanskiy, A., & Kholikov, S. 2015, ApJ, 805, 133
Kuhn, J. R. 1988, ApJ, 331, L131
Kuhn, J. R. 1993, in GONG 1992: Seismic Investigation of the Sun and Stars, ed. T. Brown (San Francisco: ASP), ASP Conf. Ser., 42, 27
Kuhn, J. R. 1998, in GONG/SoHO 6 Meeting, ed. S. Korzennik, ESA SP, 418, 418
Kuhn, J. R. 2000, Space Sci. Rev., 94, 177
Kuhn, J. R., & Stein, R. F. 1996, ApJ, 463, L117
Kuhn, J. R., & Schüssler, M. 2000, Space Sci. Rev., 94, 177
Kuhn, J. R., Libbrecht, K. G., & Dicke, R. H. 1987, Nature, 328, 326
Kuhn, J. R., Libbrecht, K. G., & Dicke, R. H. 1988, Science, 242, 908
Kuhn, J. R., Bush, R. I., Scherrer, P., & Schreick, K. 1998, Nature, 392, 155
Kuhn, J. R., Bush, R. I., Emilio, M., & Scholl, I. F. 2012, Science, 337, 1638
Lefebvre, S., & Kosovichev, A. G. 2005, ApJ, 633, 149
Libbrecht, K. G., & Woodard, M. F. 2000, Nature, 345, 779
Lites, B. W., Centeno, R., & McIntosh, S. W. 2014, PASJ, 66,1
Lydon, T. J., & Sofia, S. 1996, Phys. Rev. Lett., 76, 177
Muller, R., Hanslmeier, A., & Saldana-Munoz, M. 2007, A&A, 475, 717
Muller, R., Hanslmeier, A., & Utz, D. 2011, Sol. Phys., 274, 87
Münzer, H., Hanslmeier, A., Schröter, E. H., & Wöhl, H. 1989, A&A, 213, 431
Nagashima, K., Zhao, J., Kosovichev, A. G., & Takashi, S. 2011, ApJ, 726, 17
Parker, E. N. 1987, ApJ, 312, 868
Parker, E. N. 1995, ApJ, 440, 415
Rimmele, T., & Schröter, E. H. 1989, A&A, 221, 137
Rodriguez Hidalgo, I., Collados, M., & Vazquez, M. 1992, A&A, 264, 661
Rozelot, J. P., Damiani, C., & Pireaux, S. 2009, ApJ, 703, 1791
Tsuneta, S., Suematsu, Y., Ichimoto, K., et al. 2008, Sol. Phys., 249, 167
Weber, M. A., Fan, Y., & Miesch, M.S. 2013, Sol. Phys., 287, 239
Zhao, J., Bogart, R. S., Kosovichev, A. G., Duvall, J. R., & Hartlep, T. 2013, ApJ, 774, L29